Hyper-polarisation of xenon nuclei by spin-exchange optical pumping with broadband diode laser in an optically opaque medium

D. Radnatarov*, S. Kobtsev
Novosibirsk State University, Pirogova str., 2, Novosibirsk, Russia 630090

ABSTRACT

This study examines the efficiency of spin hyper-polarisation of xenon nuclei via spin-exchange optical pumping in an optically opaque medium of rubidium vapour with almost complete absorption of resonant radiation. A numerical model is presented that takes into account the depletion of broadband pumping in opaque medium. The study shows that the proposed method of estimating average rubidium polarisation from absorption measurements of the optical pump radiation is applicable. The authors also demonstrate theoretically and experimentally the creation of a xenon polarisation gradient in an optically opaque medium and propose a technique to maximise signal from gradient-polarised xenon in NMR spectroscopy.

Keywords: Xe hyperpolarisation, spin-exchange optical pumping (SEOP), Rb optical cell, diode laser application

1. INTRODUCTION

Hyper-polarised xenon is a promising contrast agent in NMR spectroscopy and tomography with various applications in biomedical[1] and material science[2]. Spin-exchange optical pumping (SEOP) is a widely used method for xenon polarisation, where circularly polarised radiation is absorbed by alkali metal vapour, leading to polarisation of electron spins transferred to xenon nuclei in spin-exchange collisions[3]. However, the efficiency of the polarisation process depends on several parameters, including the concentration of alkali atoms, power, and optical width of the radiation spectrum. Currently, the output spectral width of available powerful diode lasers exceeds that of the alkali metal atom absorption line, leading to quick attenuation of the pumping intensity as it propagates along the optical cell where spin polarisation takes place. This effect produces a gradient in rubidium and xenon polarisation. This problem is most acutely manifested in compact polarisers based on general-purpose broad-band diode lasers whose output spectrum is by a few orders of magnitude wider than the absorption line[4,5]. This study presents a numerical model that considers the gradual attenuation of broad-band pumping radiation as it interacts with an optically opaque medium of rubidium vapour with almost complete absorption of resonant radiation. By application of this model, it became possible to substantiate the experimental results on optimisation of the conditions for xenon polarisation in a table-top polariser based on a diode laser with an emission line-width exceeding 1 nm. From the practical viewpoint, the most interesting question is the possibility of estimation of rubidium and xenon polarisation degree without direct measurement of the NMR signal. The study shows that the earlier-proposed method of estimating average rubidium polarisation from absorption measurements of the optical pump radiation[6] is applicable to optimisation of the polarisation regime with depleted resonant part of the optical pump. The study demonstrates creation of a xenon polarisation gradient in an optically opaque medium and proposes a technique to maximise NMR signal from gradient-polarised xenon in spectroscopy

*d.radnatarov@nsu.ru

Semiconductor Lasers and Applications XIII, edited by Wei Li, Werner H. Hofmann, Ting Wang, Proc. of SPIE Vol. 12761, 1276112 · © 2023 SPIE
0277-786X · doi: 10.1117/12.2687439

2. NUMERICAL MODEL

For analysis of processes related to SEOP polarisation of xenon, a probabilistic numerical model was developed that allows estimation of how various factors affect the xenon polarisation process. The concept of the model consists in the following: the volume of the optical cell containing rubidium and xenon atoms, in which atomic polarisation occurs, is represented as a chain of clusters sequentially interacting with the photon flux (see Fig. 1). Photons have a given wavelength distribution. Each cluster contains one rubidium atom that can absorb a photon from the incident flux with a probability defined by the atomic absorption spectrum and thereby shift to the polarised state. The cluster also contains xenon atoms, each of which has a definite probability to interact with the rubidium atom and exchange spin states with it. Each of xenon and rubidium atoms may spontaneously change its state (spin relaxation). In our modelling, we used chains of up to 100,000 clusters, and each cluster could contain up to 100,000 xenon atoms.

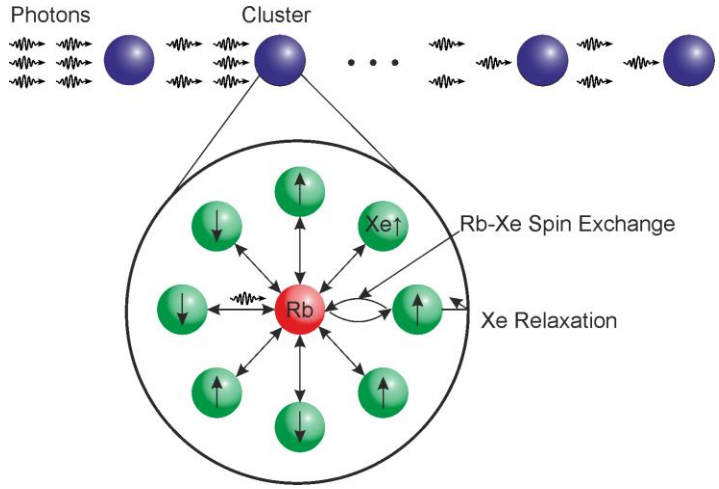

Figure 1. Numerical model diagram. Atoms in the optical cell are represented as a chain of clusters that sequentially interact with the photon beam having a given wavelength distribution. Each cluster consists of a rubidium atom surrounded by xenon atoms. The probability of photon absorption is defined by the absorption spectrum of rubidium atom and its state.

Although the presented model is very simple and does not take into account many factors, comparison of the modelling results with the experiment indicates that this model may be used for qualitative description of the major dependencies in the processes involved. In particular, this approach allows to reflect the broadening of the effective absorption line when pump radiation is depleted due to absorption of the resonant line wings[7] and to understand the distribution of the polarisation degree along the cell as the pump is gradually depleted, as well as to analyse the effect of rubidium and xenon atomic concentrations upon the processes of spin polarisation. Furthermore, the proposed approach may allow the possibility of extracting the average rubidium polarisation from the measurements of transmitted radiation power. Earlier, such an estimation was proposed in Ref[6], where the following formula was used:

$$\langle P_{Rb} \rangle = 1 - ln\left(\frac{I_{hot\,B-on}}{I_{cold}}\right) / ln\left(\frac{I_{hot\,B-off}}{I_{cold}}\right), \quad (1)$$

where $I_{hot\,B-on}, I_{hot\,B-off}$ are intensities of radiation passing through the cell with and without magnetic field, I_{cold} – is the intensity radiation passing through a cold cell (when the rubidium vapour density is minimal).

3. EXPERIMENTS AND CALCULATIONS

The optical part of the experimental installation used for study of SEOP processes is schematically presented in Fig. 1. The output of a diode laser delivering 4 W of power into a 2-nm spectral radiation line was collimated with a lens and guided into a thick-walled optical cell with the volume of 10 ml containing 100 mg of metallic rubidium. At the distal end of the cell, a metal reflector was placed that directed the radiation passing through the rubidium vapour onto a photo-detector and a spectrum analyser. The internal diameter of the cell made of borosilicate glass was 15 mm, and the optical path length from the proximal end of the cell to the reflector was about 85 mm. The laser beam diameter was equal to that

of the cell, although due to non-uniformity of the diode laser beam, the beam area did not exceed 50% of the internal cell cross-section area. The cell was enclosed in an aluminium case heated with two finger AC heaters having the total power of 250 W. The temperature was monitored with a thermistor installed inside the case. The reflector was made of a titanium alloy, the cell was sealed with a fluoro-plastic stopper, into which a needle valve was integrated. A more detailed description of the cell design is given in Ref.[4]. For gas filling, a vacuum station was used with residual pressure of 0.01 Torr and gases with purity of 99.9994%. Aside from rubidium and xenon, also nitrogen was added to the cell. This was necessary for suppression of spontaneous radiation generated by rubidium relaxation that results in its depolarisation[8]. In our experiments, partial xenon pressure of 1 atm and total pressure of 6 atm was used in the cells. Because SEOP requires circular polarisation of optical radiation and magnetic field parallel to the optical axis, a quarter-wave plate was inserted in front of the cell in the beam. The cylindrical aluminium case was used as a frame for the magnetic coil that, when powered, generated an internal field of ~ 2 mT.

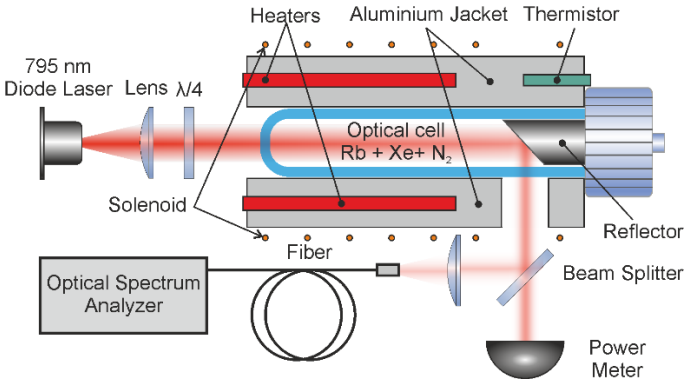

Figure 2. Scheme of the experimental setup.

Fig. 3 presents theoretical and experimental radiation spectra after interaction with the medium. From these curves, it may be seen that the model correctly describes absorption of broad-band radiation. In particular, it may be noticed that a dip in the radiation spectrum is broadened when the rubidium atom concentration becomes so high that the radiation in the centre of the line is almost completely absorbed by them.

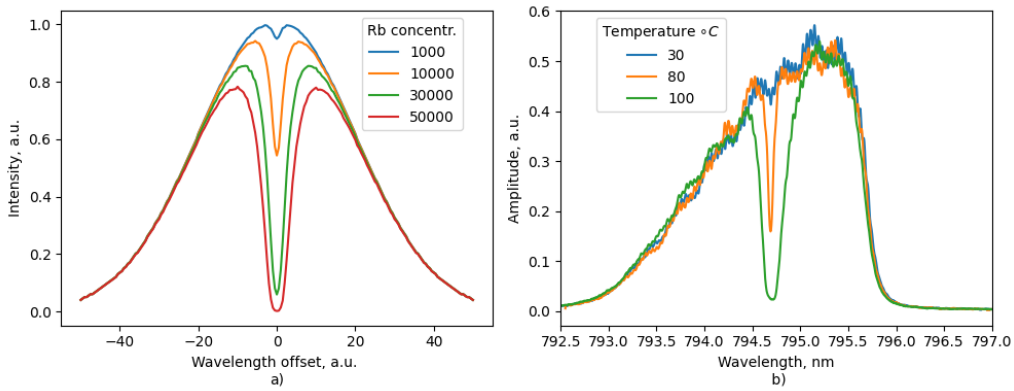

Figure 3. Radiation spectra after interaction with the medium: a) theoretical spectra at different number of clusters and fixed total number of xenon atoms; b) measured spectra at different temperatures.

Given in Fig. 4 are the theoretical dependencies of the absorption and polarisation levels of xenon and rubidium obtained directly from the model and by calculations based on the exit radiation intensity (Eq. 1) at different number of xenon atoms. This graph shows that the proposed model correctly illustrates the main features of the system behaviour. The rubidium degree of polarisation declines as the xenon concentration is raised, and the polarisation calculated by Eq. 1 is lower. That is, the value obtained from the radiation power measurements is a lower estimate of the polarisation degree. The results demonstrate that as the xenon concentration is increased, the difference between the polarisation degrees of rubidium and xenon gets smaller, thus corresponding to the results presented in Refs.[6, 9].

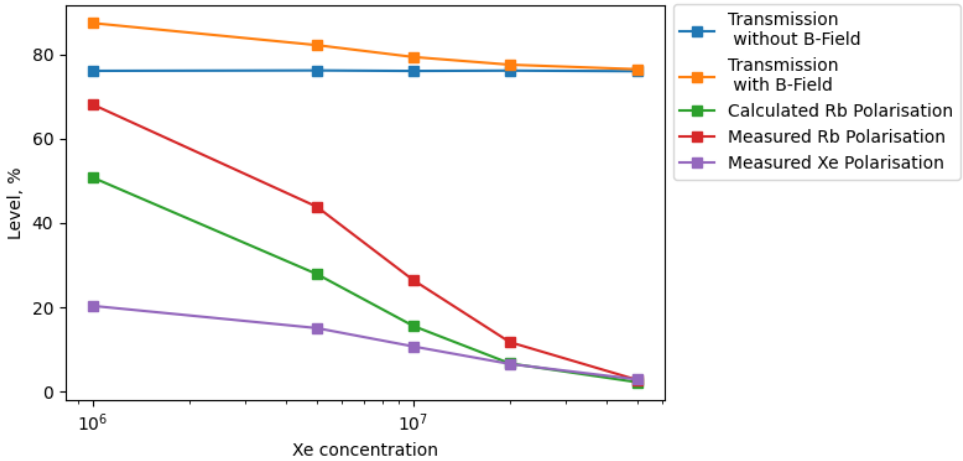

Figure 4. Parameter dependence upon xenon atom count in each cluster. Orange and blue curves are the theoretical dependences of transmittance with and without magnetic field, correspondingly. Green curve is the rubidium polarisation degree calculated with Eq. 1. Red curve is the rubidium polarisation degree from the model. Violet curve is the xenon polarisation degree from the model.

Further on, we studied the impact of the rubidium atomic concentration upon the SEOP processes. In the model, the atomic concentration was determined by the cluster chain length, whereas in experiment, it was determined by the cell temperature. The total number of xenon atoms in the entire chain and in the cell was constant. The respective results are shown in Fig. 5. It is evident from the plots that in this case, the model matches well the real behaviour of the system. Particularly, a certain optimal atomic concentration emerges, and hence, its corresponding cell temperature, at which the highest rubidium polarisation is attained (as calculated by Eq. 1). From the model, we can also extract data on degree of polarisation of rubidium and xenon (Fig. 5a), and its distribution along the chain (Fig. 6). It may be pointed out that the experimentally measured polarisation degree of rubidium exceeds the estimate and that the optimal rubidium concentration from the viewpoint of estimation by Eq. 1 corresponds to the value at which the highest average xenon polarisation is achieved. Therefore, it is reasonable to believe that the experimental polarisation degree of rubidium at 110 °C is higher than the calculated 50%, and that the average polarisation degree of xenon is at its maximum, but at the same time there may be a significant polarisation gradient of both xenon and rubidium along the cell.

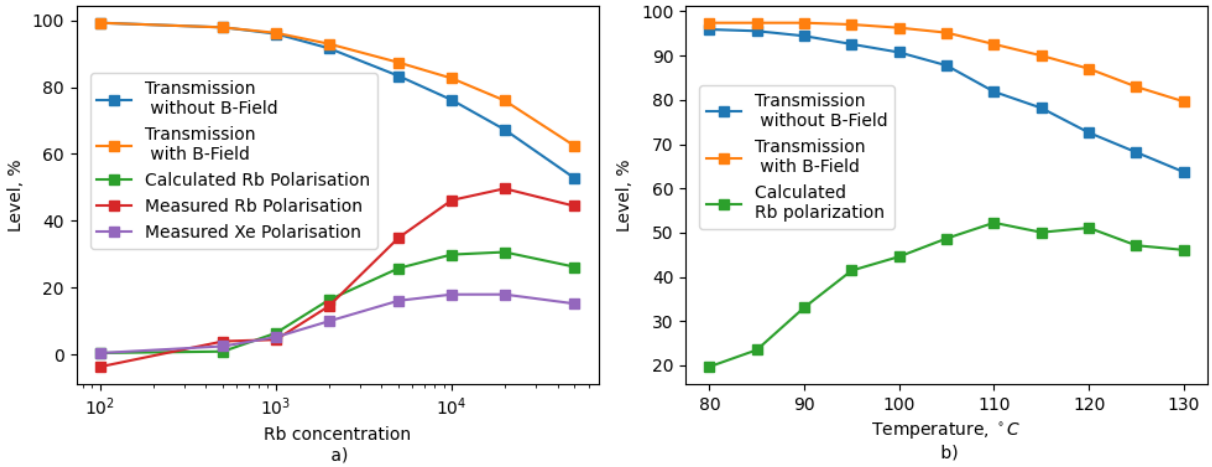

Figure 5. Dependence of absorption and polarisation degree upon the atomic rubidium concentration and cell temperature. Calculated Rb polarisation is the polarisation calculated from Eq. 1.

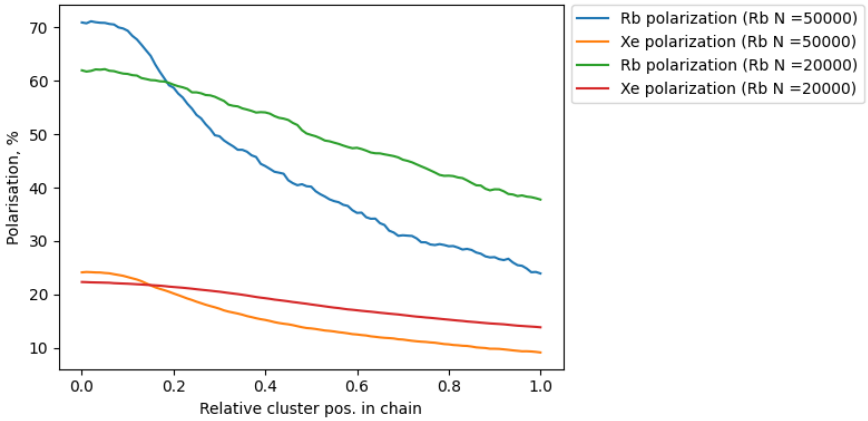

Figure 6. Profile of rubidium and xenon atomic polarisation as a function of the longitudinal coordinate in the cell.

From the practical viewpoint, we were interested in the possibility of combined use of the table-top polariser and an NMR spectrometer for developing the procedure of filling the NMR spectrometer tube and for measurement of xenon polarisation degree. For this, a prototype polariser with a set of optical cells was moved into a laboratory where an NMR spectrometer was installed with the field strength of 7 T. A schematic diagram of the experiment on practical application of the polariser is given in Fig. 7. The polariser cell and that of the NMR spectrometer were connected with thin (inner diameter within 2 mm) fluoro-plastic tubing through a three-way valve also connected to a vacuum pump. Before the experiment, the tubing was evacuated with the pump, which was then cut off. The valve of the polariser cell was opened and the gas flew into the NMR spectrometer tube, the internal pressure reaching ~ 1 atm. Following a series of experiments on measurement of xenon polarisation, the best result was 1.1%, which exceeds by a factor of 1640 the equilibrium xenon polarisation in the NMR spectrometer field. The results were calibrated to an earlier measured NMR spectrum of xenon, which was obtained with the NMR spectrometer tube filled with pure xenon at the pressure of 3.7 atm.

During a series of successive NMR spectrum measurements after filling the spectrometer tube, it was discovered that the signal strength initially increases (see Fig. 9a) even though NMR signal measurement is destructive of the non-equilibrium state of xenon nuclei, viz. the spin polarisation should be decaying. This circumstance is a consequence of a gradient in the polarisation of rubidium and xenon in the polariser cell, which leads to accumulation of xenon gas with lower polarisation degree in the measurement area at the bottom of the spectrometer tube, while stronger polarised gas remains at the top. As the gas layers slowly mix up, the NMR signal gradually increases.

In order to eliminate such an effect of polarisation gradient, a thin capillary (see Fig. 8) was placed inside the spectrometer tube that delivered the polarised gas at the bottom. Now the first weaker polarised portion of the gas entered the first and then was displaced towards the top by stronger polarised gas. In this implementation, the highest signal was detected in the first measurement and then it gradually decayed. (see Fig. 9b).

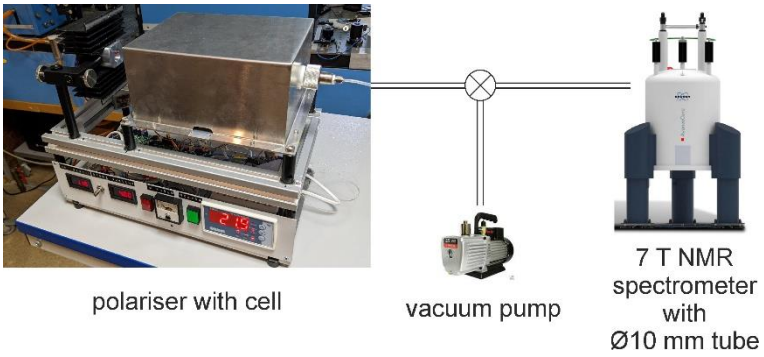

Figure 7. Schematic diagram of the experiment on NMR spectroscopy of polarised xenon.

Figure 8. NMR tubes a) standard 10 mm in diameter tube b) tube with PTFE capillary

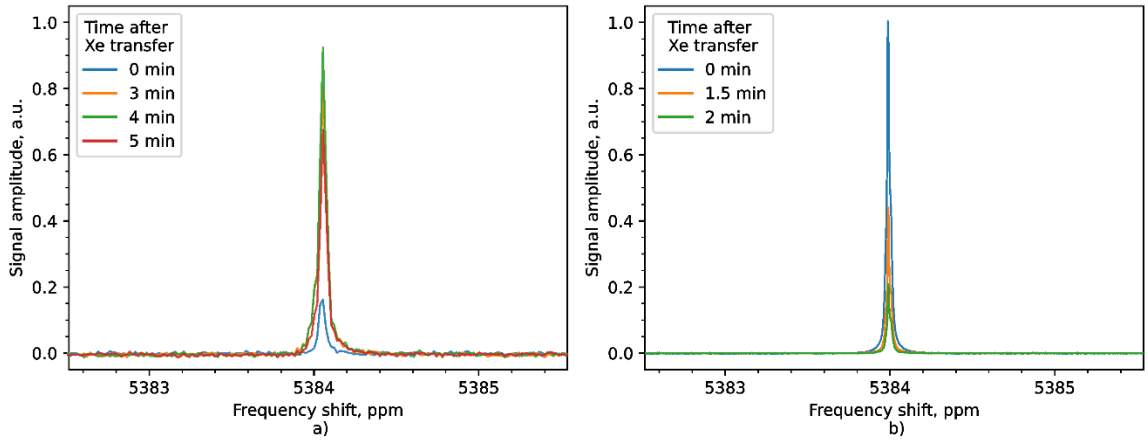

Figure 9. NMR signals measured at different moments of time after filling the NMR spectrometer tube with gas. a) standard tube; b) tube with a capillary.

It may be remarked that inserting a capillary into the spectrometer tube prevents collecting the most strongly polarised gas from the polariser cell. This is why the experiments presented here did not attain the highest possible level of the NMR signal. Nevertheless, the 1% level of xenon polarisation is sufficient in a number of practical applications, including characterisation by NMR methods of metal-organic frameworks and other porous compounds.

4. CONCLUSION

As a result of the conducted research, we proved efficiency of spin hyper-polarisation of xenon nuclei by spin-exchange optical pumping in optically opaque rubidium vapour medium where almost total absorption of resonant radiation is observed. A numerical model of the polarisation process was developed that takes into account depletion of broad-band pumping radiation in interaction with optically opaque medium. The present research has confirmed validity of the approach to estimation of the average volumetric rubidium polarisation relying on measurements of changes in the medium absorption caused by the effect of optical pumping. It was also theoretically substantiated and experimentally demonstrated that a xenon polarisation gradient is created in an optically absorbing medium. In the course of this work, a method of maximisation of the signal generated by xenon polarised with a gradient was proposed for NMR spectroscopy. The produced results usher in new opportunities for development of SEOP polarisers based on common broad-band diode lasers, first of all for table-top systems used in applications of NMR spectroscopy.

5. ACKNOWLEDGEMENTS

The work of D. Radnatarov (initial idea, experimental studies, processing of the results) was supported by a grant of the Russian Science Foundation (grant 22-22-00264). The work of S. Kobtsev (data analysis, conception and writing of the article text) was supported by the Ministry of Science and Higher Education of the Russian Federation (FSUS-2020-0036).

REFERENCES

[1] Grist, J. T., Collier, G. J., Walters, H., Kim, M., Chen, M., Abu Eid, G., Laws, A., Matthews, V., Jacob, K., et al., “Lung Abnormalities Detected with Hyperpolarized ^{129}Xe MRI in Patients with Long COVID,” Radiology **305**(3), 709–717 (2022).

[2] Fan, B., Xu, S., Wei, Y.., Liu, Z., “Progresses of hyperpolarized ^{129}Xe NMR application in porous materials and catalysis,” Magn. Reson. Lett. **1**(1), 11–27, Elsevier Ltd (2021).

[3] Walker, T. G.., Happer, W., “Spin-exchange optical pumping of noble-gas nuclei,” Rev. Mod. Phys. **69**(2), 629–642 (1997).
[4] Radnatarov, D., Kobtsev, S. M.., Andryushkov, V., “Benchtop ^{129}Xe optical polarizer for NMR applications,” Proc. SPIE(September 2022), R. Katayama and Y. Takashima, Eds., 23, SPIE (2022).
[5] Radnatarov, D.., Kobtsev, S., “Effect of absorption oscillation of resonant radiation observed in a compact installation for hyper-polarization of ^{129}Xe,” J. Opt. Soc. Am. B **40**(1), 151 (2023).
[6] Nikolaou, P., Coffey, A. M., Walkup, L. L., Gust, B. M., Whiting, N., Newton, H., Barcus, S., Muradyan, I., Dabaghyan, M., et al., “Near-unity nuclear polarization with an open-source ^{129}Xe hyperpolarizer for NMR and MRI,” Proc. Natl. Acad. Sci. **110**(35), 14150–14155 (2013).
[7] Walker, T. G., “Fundamentals of spin-exchange optical pumping,” J. Phys. Conf. Ser. **294**(1) (2011).
[8] Lancor, B.., Walker, T. G., “Effects of nitrogen quenching gas on spin-exchange optical pumping of He^3,” Phys. Rev. A - At. Mol. Opt. Phys. **82**(4), 1–7 (2010).
[9] Nikolaou, P., Coffey, A. M., Walkup, L. L., Gust, B. M., Lapierre, C. D., Koehnemann, E., Barlow, M. J., Rosen, M. S., Goodson, B. M., et al., “A 3D-printed high power nuclear spin polarizer,” J. Am. Chem. Soc. **136**(4), 1636–1642 (2014).
[10] Carter, W. H., “Focal shift and concept of effective Fresnel number for a Gaussian laser beam,” Appl. Opt. **21**(11), 1989 (1982).